



Revisiting ocean carbon sequestration by direct injection: A global carbon budget perspective

Fabian Reith¹, David P. Keller¹, Andreas Oschlies¹

¹Geomar Helmholtz-Centre for Ocean Research Kiel, Düsternbrooker Weg 20, 24105 Kiel, Germany

5 *Correspondence to:* Fabian Reith (FReith@geomar.de)

Abstract.

In this study we look beyond the previously studied effects of oceanic CO₂ injections on atmospheric and oceanic reservoirs, and also account for carbon cycle and climate feedbacks between the atmosphere and the terrestrial biosphere. Considering these additional feedbacks is important since backfluxes from the terrestrial biosphere to the atmosphere in response to reducing atmospheric CO₂ can further offset the targeted reduction. To quantify these dynamics we use an Earth-system model of intermediate complexity to simulate direct injection of CO₂ into the deep ocean as a means of emissions mitigation during a high CO₂ emission scenario. In three sets of experiments with different injection depths, we simulate a 100-year injection period of a total of 70 GtC and follow global carbon cycle dynamics over another 900 years. Simulated seawater chemistry changes and marine carbon storage effectiveness are similar to previous studies. As expected, by the end of the injection period avoided emissions fall short of the targeted 70 GtC by 16% to 30% as a result of carbon cycle feedbacks and backfluxes in both land and ocean reservoirs. An unexpected feature are effects of the model's internal variability of deep-water formation in the Southern Ocean, which, in some model runs, causes additional oceanic carbon uptake after injection termination relative to a control run without injection and therefore with slightly different atmospheric CO₂ and climate. These results of a model that has very low internal climate variability illustrate that attribution of carbon fluxes and accounting for injected CO₂ may be very challenging in the real climate system with its much larger internal variability.



1. Introduction

25 Anthropogenic CO₂ emissions have perturbed the natural carbon cycle [Archer et al., 2009]. With an average of 8.6 ± 0.4 GtC yr⁻¹ emitted from fossil-fuel burning and 0.8 ± 0.5 GtC yr⁻¹ from land-use change in the last decade (2003 – 2013) [Le Quéré et al., 2014], global CO₂ emissions have continuously increased by about 2.5 % yr⁻¹ [Friedlingstein et al., 2014]. This trend continues to follow slightly above the trajectory of the highest emission scenario of the latest IPCC report (see section 2.2), which makes it very difficult to keep global warming within the political 2°C guardrail [Peters et al., 2013], not
30 to speak of recent agreements to seriously consider an even more ambitious 1.5°C goal [UNFCCC, 2015]. The limited success in reducing or even slowing down the increase in anthropogenic emissions through global climate accords [Rogelj et al., 2010] has led to renewed interest in engineering measures that are intended to reduce atmospheric CO₂ concentrations [e.g., Shepherd, 2009].

Marchetti [1977] proposed directly injecting CO₂ into the deep ocean, thus accelerating the oceanic uptake of
35 atmospheric CO₂, which happens naturally via invasion and subsequent dissolution of CO₂ into the surface waters, albeit at a relatively slow rate limited by the sluggish ocean overturning circulation. On time scales of thousands of years, however, this will result in most anthropogenic CO₂ ending up in the deep ocean. The idea behind direct CO₂ injection is to speed up this slow natural process by directly depositing CO₂ in deep waters, some of which remain isolated from the atmosphere for hundreds to thousands of years [DeVries and Primeau, 2011; their Figure 12], thereby preventing the CO₂ from having an
40 effect on the climate in the near future. This is fundamentally different from just avoiding emissions, because the CO₂ has still been added to the carbon cycle and may leak out of the ocean and affect the climate and other carbon cycle pathways.

Over millennial time scales carbon from direct injection can simply be viewed as "delayed" emissions, in terms of its climatic effect and fate, since the carbon cycle will eventually reach a chemical equilibrium (mainly an equilibrium between the ocean and atmospheric carbon reservoirs). However, on decadal to centennial time scales, carbon that is
45 sequestered via direct injection cannot simply be treated as "delayed emissions" because the injected carbon must take fundamentally different pathways than that of carbon that is emitted directly into the atmosphere. Since these pathways operate on many different timescales and are partially controlled by climate feedbacks, it takes a considerable amount of time until the carbon cycle and climate reach the same state as if the emissions had just been delayed. This is because



injecting CO₂ changes ocean chemistry internally and thus, will at some point affect ocean carbon uptake or outgassing, and
50 hence the atmospheric CO₂ concentration, when the water whose chemical properties have been altered by the injection
reaches the surface, i.e., the air-sea exchange of CO₂ is fundamentally altered by this method in a manner that is quite
different than if the carbon was just emitted into the atmosphere at a later date. By sequestering carbon in the ocean instead
of emitting it into the atmosphere, it also inadvertently affects terrestrial carbon cycling if the comparison is made to the
situation where the carbon was emitted.

55 Because direct injection of CO₂ is presently in conflict with the London Protocol and the Convention for the
Protection of the Marine Environment of the North East Atlantic (OSPAR Convention) [Leung et al., 2014], and due to the
long timescales and global scales involved, models are ideally suited for investigating this method [Orr, 2004]. In previous
studies, relatively simple box models [e.g., Hoffert et al., 1979] and first-generation global ocean circulation models [Orr,
2004] were employed, focusing on the residence time of the injected CO₂ (i.e. effectiveness), as well as on changes in ocean
60 chemistry [e.g., Orr et al., 2001; Orr 2004; Jain and Cao, 2005; IPCC, 2005; Ridgwell et al., 2011]. However, a more
comprehensive assessment of the carbon sequestration and climate mitigation potential of direct injection also requires
accounting for the changes in all ambient carbon fluxes resulting from carbon cycle and climate feedbacks [Mueller et al.,
2004; Vichi et al., 2013].

In this study, which follows Orr et al. [2001] in the configuration of the CO₂ injection scenarios, we use an Earth
65 system model of intermediate complexity and fully interactive carbon cycle to simulate the direct injection of CO₂ into the
deep ocean at different depths under a high CO₂ emission scenario. Our main objective is to assess the long-term response of
the atmospheric, oceanic and terrestrial carbon pools to the targeted atmospheric reduction through a continuous 100-year
injection of CO₂ at seven offshore sites with individual injection rates (0.1 GtC yr⁻¹ each) that are small compared to today's
global CO₂ emissions. Although previous studies [e.g., Orr et al., 2001; Orr 2004] have looked at the effects of CO₂
70 injections on atmospheric and oceanic reservoirs, the carbon-cycle and climate feedbacks between the atmosphere and the
terrestrial biosphere were not considered in those studies because their models used did not have a land component.
Considering these feedbacks is important since simulations of other oceanic carbon sequestration methods have shown that
backfluxes from the terrestrial biosphere to the atmosphere can partially offset any oceanic C uptake [Oschlies et al., 2010].



75 For our injection simulations we use a well-calibrated model that conserves carbon globally, features the pelagic carbonate chemistry and is run under a business as usual emission scenario. The model and emission forcing used are identical to the ones in the Climate Engineering modeling study by Keller et al. [2014].

2. Methodology

2.1 Model Description

80 The model used is version 2.9 of the University of Victoria Earth System Climate Model (UVic ESCM). It consists of four dynamically coupled components: a three-dimensional general circulation ocean model (Pacanowski, 1996), a dynamic-thermodynamic sea-ice model (Bitz and Lipscomb, 1999), a terrestrial model [Meissner et al., 2003], and a one-layer atmospheric energy-moisture balance model [based on Fanning and Weaver, 1996]. All components have a common horizontal resolution of 3.6° longitude x 1.8° latitude. The oceanic component has 19 vertical levels with thicknesses ranging from 50 m near the surface to 500 m in the deep ocean. Formulations of the air-sea gas exchange and seawater carbonate
85 chemistry are based on the OCMIP abiotic protocol [Orr et al., 1999]. The terrestrial model of vegetation and carbon cycles is based on the Hadley Center model TRIFFID. A more detailed description of the UVic model version used here is given in Keller et al. [2012] and Eby et al. [2013].

2.2 Experimental Design

90 The model has been spun-up for 10,000 years under preindustrial atmospheric and astronomical boundary conditions and run from 1765 to 2005 using historical fossil fuel and land-use carbon emissions (Keller et al., 2014). From the year 2006 to 2100 the model is forced with CO_2 emissions following the Representative Concentration Pathway (RCP) 8.5, which is a business-as-usual high CO_2 emission scenario. Subsequently, simulations follow the Extended Concentration Pathway (ECP) 8.5 emission scenario until the year 2500 [Meinshausen et al., 2011]. Thereafter, we keep emissions constant at 1.48 GtC yr^{-1} until the end of the simulations in year 3020.

95 Continental ice sheets, volcanic forcing and astronomical boundary conditions are held constant to facilitate the experimental setting and analyses (e.g., to prevent confounding feedback effects) [Keller et al., 2014]. Parameterized



geostrophic wind anomalies, which are a first-order approximation of dynamical feedbacks associated with changing winds in a changing climate (Weaver et al., 2001), are also applied.

100 Simulated CO₂ injections into different ocean regions are based on the Ocean Carbon Cycle Model Intercomparison Project (OCMIP) carbon sequestration protocols [see Orr et al., 2001; Orr 2004] to facilitate comparison of our model results to those of Orr et al. [2001] and Orr [2004]. For simplicity, we simulate the injection of CO₂ in an idealized manner by adding CO₂ directly to the dissolved inorganic carbon (DIC) pool [Orr, 2001], thus neglecting any gravitational effects and assuming that the injected CO₂ instantaneously dissolves into seawater and is transported quickly away from the injection point and distributed homogeneously over the entire model grid box with lateral dimensions of a few hundred kilometers and
105 many tens of meters in the vertical direction. Consequently, the formation of CO₂ plumes or lakes is neglected. To track the physical transport of the injected CO₂ and its transport pathways, we simultaneously add site-specific diagnostic marker tracers with the injected CO₂. In all of our injection simulations we subtract the amount of injected CO₂ from the emissions forcing, thus keeping the total global carbon inventory the same as in the respective control simulation without CO₂ injection. For the purpose of assessing how all ambient carbon fluxes affect the storage lifetime of the injected CO₂, it is
110 essential to have the same carbon inventory in all of our simulations. Following Orr et al. [2001] and Orr [2004], seven injection sites are located in individual grid boxes near the Bay of Biscay (42.3°N, 16.2°W), New York (36.9°N, 66.6°W), Rio de Janeiro (27.9°S, 37.8°W), San Francisco (31.5°N, 131.4°W), Tokyo (33.3°N, 142.2°E), Jakarta (11.7°S, 102.6°E) and Mumbai (13.5°N, 63°E) (Fig. 1). Starting in the year 2020, the experimental simulations consist of two periods: 1) an initial 100 year period of simultaneous 0.1 GtC yr⁻¹ injections and 2) a continuation of the model simulations until year 3020 after
115 stopping the injections at the end of year 2119. Separate injection (I) experiments following this protocol are conducted at three different depths, 850 m (I-800), 1600 m (I-1500), and 2900 m (I-3000). Hereafter, these are referred to as With Emissions (WE) simulations.

Following previous studies [e.g., Jain and Cao, 2005; Ridgwell et al., 2011] additional simulations are conducted to investigate how climate-change induced feedbacks affect the fate of injected CO₂. These simulations follow the same
120 protocols described above, but with anthropogenic emissions forcing set to zero from the year 2020 until the end of the simulations (year 3020). Hereafter, these extreme scenarios are referred to as Complete Mitigation (CM) simulations. Note



that since these simulations are forced with historical emissions and the RCP 8.5 scenario until year 2020, the model is not in steady state in 2020 and some climatic change occurs. Also, because the injected CO₂ is withdrawn from the atmosphere so that total carbon is conserved, the CM injection runs essentially have negative emissions of 0.7 GtC yr⁻¹.

125 To determine how long the injected carbon stays in the ocean, we follow the IPCC [2005] and calculate a fraction retained ($FR = M_o * M_i^{-1} * 100$), which is the percentage ratio between the total mass of the injected carbon that remains in the ocean (M_o , determined using the diagnostic marker tracer) and the total cumulative mass injected into the ocean (M_i) since the start of the injection period (year 2020). This metric accounts for the injected carbon atoms and does not include possible adjustments of fluxes of other carbon in the Earth system.

130 To assess the global carbon cycle response to the injections, we use another metric, the net fraction stored ($netFS = \Delta C_{ocean} * M_i^{-1} * 100$, in %) that measures total carbon reservoir changes. The *netFS* is defined as the ratio between the absolute change in globally integrated total oceanic carbon (ΔC_{ocean}), relative to the RCP 8.5 control run, and the total cumulative mass injected into the ocean (M_i) since the start of the injection period. In contrast to *FR* that counts only the injected carbon atoms, *netFS* accounts for all potential feedbacks of carbon fluxes into and out of the ocean in response to
135 the injection of CO₂ into the ocean.

To investigate if the targeted atmospheric carbon reductions in the WE simulations, differ from what would happen if CO₂ was never emitted (avoided emissions) or first emitted and subsequently removed from the atmosphere, e.g., via technology such as direct air capture (DAC, see section 3.4.1) [Lackner, 2009] and subsequent safe and permanent storage, presumably in geological reservoirs, we performed another simulation where the atmospheric CO₂ concentration was 0.7
140 GtC yr⁻¹ less than in the RCP 8.5 control run between the years 2020 and 2120. Hereafter, this simulation is referred to as DAC run.

3. Results and Discussion

3.1 RCP 8.5 control simulation

The physical climate and biogeochemical cycles of the Earth System during the RCP 8.5 control simulation are in
145 the same state as described in Keller et al. [2014]. Here, we briefly describe global carbon cycling during the control simulation so that comparisons can be made to the WE simulations (section 3.4).



By the end of the simulation in year 3020, about 6,000 GtC have been added to the global carbon cycle. Consequently, atmospheric CO₂ has increased substantially, leading to a total atmospheric carbon content of about 4620 GtC at the end of the simulation (Figs. 2 a, b).

150 By the end of the extended RCP8.5 control run about 58 % of the emitted CO₂ remains in the atmosphere. The rest of the carbon has been taken up by oceanic and terrestrial reservoirs (Figs. 2 d, f). Oceanic carbon uptake is highest during the first few decades of the simulation, when emissions are highest, and then decreases thereafter (Fig. 2 c). The decrease in net oceanic carbon uptake is particularly caused by a reduction in the ocean buffering capacity [Prentice et al., 2001], leading to a decrease in ocean carbon uptake even under increasing atmospheric CO₂ levels; a response also seen in other model
155 simulations [Zickfeldt et al., 2013].

Simulated terrestrial carbon uptake is initially high as well, but then declines rapidly, with the terrestrial reservoir becoming a source for atmospheric carbon in the year 2139 before leveling off at very little net exchange between the terrestrial reservoir and the atmosphere after about year 2280 (Fig. 2 e). The initial increase in total land carbon uptake is due to the simulated CO₂ fertilization effect on vegetation [Matthews, 2007]. However, as temperatures become higher,
160 terrestrial net primary productivity (NPP) is reduced due to water stress. Moreover soil respiration increases with temperature until it eventually becomes the dominant processes, leading to a net loss of carbon from the terrestrial reservoir to the atmosphere. Projections of future net terrestrial carbon uptake or loss processes are highly uncertain (Carvalhais et al., 2014; Hagerty et al., 2014; van der Sleen et al., 2014; Sun et al., 2014), which is also reflected in the large variability between the CMIP5 (Coupled Model Intercomparison Project Phase 5) model results, with changes in terrestrial carbon
165 budgets ranging from -0.97 to +2.27 GtC yr⁻¹ between 2006 and 2100 [Ahlström et al., 2012].

3.2 Changes in seawater chemistry

Here, we compare the WE simulations to the RCP 8.5 control run to assess injection-related seawater chemistry changes. By the final year of the injection period (year 2119), a total of 10 GtC is injected at each site (Fig. 1). The respective increases in DIC and reductions in pH depend on how quickly the injected carbon is transported away from the
170 injection sites by local ocean currents and mixing [see Orr, 2004]. Our model-predicted changes in DIC and pH at the injection sites (relative to the control run) are within the range of Orr [2004] (Table S1-2).



Simulated ocean surface pCO₂ is lower in the CO₂ injection runs because of lower atmospheric CO₂ levels and the related decrease in air-sea carbon fluxes, which results in lower surface DIC concentrations and a slightly higher surface pH (by 0.008 to 0.01 units compared to the control run).

175 3.3 Fractions retained

Here, we assess to which extent the simulated CO₂ injections are effective in keeping the injected carbon out of the atmosphere. This is described by the fractions retained (*FR*). The global *FR* of our CM and WE simulations (Table 1) are within the full range of the GOSAC-OCMIP results [Orr et al., 2001; Orr, 2004]. The simulated *FR* (Table 1) increases with the depth of injection because it generally takes longer for deeper waters to again come into contact with the atmosphere, something also shown in previous studies [e.g., Caldeira et al. 2001; Orr et al., 2001; Orr, 2004; Jain and Cao, 2005].

By comparing the WE and CM simulations at all depths, we can determine how climate change affects *FR*. As in previous studies, our results show that *FR* is enhanced by climate change [Jain and Cao, 2005; Ridgwell et al., 2011]. In the WE simulations values of *FR* are always higher than in the CM runs (Table 1). For I-800 and I-1500, the *FR* increase due to climate change is largest in the Pacific, whereas for I-3000, Atlantic sites show the highest *FR* increase due to a larger ocean response to climate change (Table 1). However, in all simulations more of the injected carbon is retained in the Pacific compared to injections in other ocean basins.

We also assess whether the enhanced *FR* in our WE simulations are affected by changes in the Atlantic Meridional Overturning Circulation (AMOC). Relative to preindustrial, which has a maximum AMOC intensity of 15.98 Sv, we find AMOC decreases by 8%, 29%, 40%, 34% in the years 2020, 2120, 2520, 3020, respectively in the WE simulations. AMOC in the CM simulations, relative to preindustrial, shows smaller decreases of about 7.6%, 21%, 8.6%, 8.6% in the years 2020, 2120, 2520, 3020, respectively. These differences partially explain why *FR* is enhanced in the WE simulations, since a reduced AMOC slows the transport of deep water masses and prolongs the time until they again come into contact with the atmosphere. As in other climate change studies [e.g., Doney, 2010; Bopp et al., 2013], we also find an increase in ocean stratification (not shown) in all respective basins in our WE runs, relative to the CM runs, which has also led to reduced vertical mixing [Prentice et al., 2001] and increased *FR*. In contrast to Jain and Cao [2005], who found a higher *FR* mainly in



the Atlantic, we find a higher FR in all basins (Table 1). This difference is likely related to the higher degree of climate change in our simulations since we use a higher CO_2 emissions scenario.

Model-predicted FR (Table 1) refers to the injected CO_2 alone (as accounted for by the diagnostic marker tracer) and does not account for how global carbon cycle feedbacks affect net ocean carbon storage. By comparing FR and net fraction stored ($netFS$, see section 2.2) for the WE simulations, we find that net ocean C sequestration is less efficient than would be predicted from FR alone (Fig. 4 a) because of carbon cycle and climate feedbacks (Fig. 1). For I-3000, $netFS$ is about 16% lower than FR at the end of the injection period (Table 1, Fig. 4 a). These results show the importance of accounting for carbon cycle feedbacks when assessing the effectiveness of marine CO_2 injections. Interestingly, an exception occurs for the I-1500 simulation from the last year of the injection period with a Southern Ocean deep convection event during which the ocean temporarily takes up more carbon than would be expected from the injections alone (Figs. 4 a, c, d). This event and its implications for carbon accounting are discussed in more detail in section 3.4.2.

3.4 Response of the Global Carbon Cycle

Here we first briefly show how the atmospheric carbon reduction, relative to the RCP8.5 control run (see section 3.1), differs between WE simulations and the DAC run. Subsequently, we investigate how carbon cycle and climate feedbacks affect the distribution of carbon between different reservoirs upon injection of CO_2 in the WE simulations. To do so, we look at the absolute changes in carbon between the WE simulations and RCP 8.5 control run during and after the injection period.

3.4.1 Response during injection period

In the WE simulations and the DAC run, the globally injected carbon (GIC) denotes the targeted atmospheric carbon reduction. The GIC - in the absence of leakage and backfluxes - equals the oceanic carbon addition or atmospheric CO_2 removal of 70 GtC by the last year of the injection period (year 2119). As presented in Figures 3, 4 b, the atmospheric carbon reduction during the injection period of the WE simulations diverges quickly from the GIC trajectory.

This is explained by injected carbon leaking from the ocean back to the atmosphere and the response of atmosphere-to-land and atmosphere-to-ocean fluxes to the reduction in atmospheric carbon. The rapid divergence even for the deepest injection



220 points where FR is high, points to carbon cycle and climate feedbacks, which are directly related to changes in atmospheric
CO₂ concentrations (i.e. ocean-atmosphere pCO₂ differences and CO₂ fertilization effects) and changes in temperature. Other
studies have also shown that these feedbacks occur and affect the size of the global carbon reservoirs (Arora et al., 2013).
The curve progression of the atmospheric reduction in the DAC run is very similar for I-1500 and I-3000, which is due to the
occurrence of most of the same carbon cycle and climate feedback mechanisms. However, due to no carbon injections in the
225 DAC run, the atmospheric reduction is higher as soon as injected carbon starts leaking in the WE simulations as presented in
Figure 3. In the UVic model (version 2.9), the atmospheric carbon reduction of the DAC run (Fig. 3) can also be referred to
as the true atmospheric carbon reduction target. Depending on depth of injection, this implies further that direct injection of
CO₂ would not be able to be 100% efficient and provide 100% of the true atmospheric reduction target on decadal to centennial
timescales (Fig. 3). Due to the occurrence of an ocean deep convection event in the DAC run after the year 2120 (see section
230 3.4.2), we cannot easily compare the DAC run to the WE simulations after the injection period.

While ocean feedbacks in response to CO₂ injection and reduced atmospheric CO₂ levels have been discussed
extensively in previous studies [e.g. Orr 2004; IPCC, 2005, Ridgwell et al., 2011], we here additionally consider land
feedbacks with the purpose of accounting for the entire Earth system's response to potential marine CO₂ injections.

By the last year of the injection period (year 2119), I-800 shows the highest divergence from GIC (Fig. 4 c) with an
235 atmospheric carbon reduction of only 48 GtC, which is 22 GtC less than targeted. Since from the dye tracer it is known that
25% (i.e. 17.8 GtC) of the injected CO₂ has leaked to the atmosphere (Table 1), C-cycle and temperature feedbacks must be
responsible for the other 4.2 GtC that remained in the atmosphere. This remaining amount can partially be explained by the
reduced pCO₂ difference between the atmosphere and the ocean, which leads to a smaller carbon flux into the ocean (Fig. 4
d). Plus, relative to the control run, there is a lower atmosphere-to-land carbon flux until approximately the year 2075 (Fig. 4
240 f), leading to 1.2 GtC less total land carbon by the end of the injections (Fig. 4 e). After the injections start (year 2020), both
NPP and soil respiration are lower in I-800 than in the control run, leading to a maximum reduction in land carbon of about
4.2 GtC in year 2075 (Fig. 4 e). Thereafter, total land carbon in I-800 increases. By the end of the injections in year 2120, the
terrestrial carbon pools have taken up 1.2 GtC less than the control run without CO₂ injection.

Roughly similar patterns are found for injection simulations I-1500 and I-3000 during the injection period, although



245 with less outgassing occurring for the deeper injections (Fig. 4 c), which led to a slightly larger reduction in terrestrial carbon uptake by the last year of the injection. Thus, the largest reduction in total atmospheric carbon with 60 GtC was found for I-3000, followed by I-1500 with 58 GtC by the end of the injection period (Fig. 4 b).

Our results suggest that the terrestrial response due to the atmospheric carbon reduction is mainly governed by the reduced CO₂ fertilization effect on NPP and the temperature related decrease in soil respiration. Carbon cycle-climate
250 feedbacks on land occur because the reduced atmospheric CO₂ concentration in the WE simulations (Fig. 4 c) leads to a cooling in the global mean soil temperature of about 0.08°C to 0.1°C in the year 2119 relative to the control simulation, with the lowest reduction for I-800 and the highest one for I-3000. Both fertilization and temperature feedbacks on the terrestrial biosphere act simultaneously, although our results indicate that the reduced CO₂ fertilization effect, which, in current models
255 land carbon around year 2075. Thereafter, the decrease in soil respiration leads to an increase in land carbon and becomes the dominant feedback.

Feedbacks from the terrestrial system to atmospheric CO₂ are among the largest uncertainties to projections of future climate change (Schimel et al., 2015). According to our analysis, these would impact our ability to predict the net carbon storage associated direct injection of CO₂ into the deep ocean.

260 3.4.2 Response after injection period

After the injections are stopped (end of year 2119), I-800 shows a continuous outgassing of about 40 GtC until the end of the simulation, which is represented by the steady divergence from GIC (Figs. 4 b, c). As in the control simulation, the terrestrial system in I-800 becomes a source of carbon between the years 2139 and 2280, although the flux is slightly lower because of lower atmospheric CO₂ and lower temperatures. Thus, the net effect is an increase in land carbon relative to
265 the control simulation with a maximum of 3 GtC in the year 2239 (Fig. 4 e). Thereafter, total land carbon in I-800 converges towards that of the RCP 8.5 control run, but remains higher until the end of the simulation (Fig. 4 e).

Unlike I-800, I-3000 actually gets closer to the GIC trajectory after the end of the injection period until the year 2199, with about 64 GtC less total atmospheric carbon than in the control simulation, compared to about 60 GtC at the end of the injection period in year 2119 (Fig. 4 b). This is a result of the reduced carbon flux from the atmosphere to the ocean,



270 relative to the RCP 8.5 control run (Fig. 4 d), with only about 4 GtC leaving the ocean by year 2199. Moreover, the land
turns from a sink into a net source of CO₂ in year 2139 (Fig. 4 f). Subsequently, I-3000 shows a steady outgassing of the
injected CO₂ from the year 2199 until the end of the simulation (Fig. 4 e), with little change in the terrestrial carbon pool
(Fig. 4 f). The processes that govern changes in terrestrial carbon in I-3000 are the same as for I-800, although more carbon
is retained in the soils resulting from lower soil temperatures in I-3000. The relatively small responses of the terrestrial
275 biosphere to the injections, compared to the RCP 8.5 control run, show a similar progression, although with different
amplitudes, as illustrated in Figure 4 f, e. After the injection period, this is especially reflected by the apparent synchronous
increase in land carbon around the year 2600 and the synchronous decrease around the year 2770 (Fig. 4 e). This is a result
of a slightly different phase of small variations in the total land carbon content of the control run (Figs. 4 g, S1 a, b), which is
the only simulation that has not seen any atmospheric CO₂ reduction. However, due to the same amount of atmospheric
280 carbon being removed and injected into the ocean, the WE runs have a similar climatic state throughout the simulations with
comparable changes in global mean air and soil temperatures (between 0.1% to 0.3% less) and precipitation over land
(between 0.1% to 0.4% more) when compared to the control run (Figs. S2 a, b, e). The high synchronicity (Fig. 4 e) can be
further explained by the fact that in the WE simulations the same biome regions are sensitive to the changes in temperature
(Figs. S2 a, b), although the magnitudes of the absolute changes in land carbon differ between the injection runs (Figs. S3-
285 S5). These regions are predominantly located at transition zones of different plant functional types that are in competition
which each other and thus shift from one to another, leading to small changes in land carbon. The offset between I-800 and I-
3000 (Fig. 4 e) is caused by higher soil respiration in I-800 (Fig. S3 d), which is due to slightly higher global mean air and
soil temperatures (Fig. S2 a, b).

For I-1500, an unexpected oceanic carbon uptake event is observed from the last year of the injection period (Figs.
290 4 c, d). This is caused by a large temporary carbon flux from the atmosphere into the ocean (Fig. 4 d), with a total of ~13
GtC taken up in a region of the Southern Ocean (~ 0°: 20°E; 60°: 70S°) between the years 2119 and 2209 (Fig. S5). Because
this event is not simultaneously present in the reference simulation without injection, the difference in atmospheric carbon
between run I-1500 and the reference run even exceeds the GIC between the years 2189 and 2262 (Fig. 4 b). For standard
accounting of carbon removed from the atmosphere with respect to a reference simulation, this would correspond to



295 sequestration effectiveness greater than 100%. The oceanic *netFS* is just less than 100% of the GIC (Fig. 4 c). Our analysis
for I-1500 suggests that the regional carbon uptake is due to an intermittent ocean deep convection event that occurs in the I-
1500 simulation. Using an earlier version of the UVic model (version 2.8), Meissner et al. [2007] found that under a CO₂
concentration of 440 ppm or higher, the modeled climate system started oscillating between a state with open-ocean deep
convection in the Southern Ocean, causing massive bottom water formation, and a state without. In their runs, which were
300 spun up to equilibrium under constant atmospheric CO₂, the simulated deep convection event led to a rapid increase in
atmospheric temperatures, carbon outgassing and a subsequent increase in atmospheric CO₂ concentrations. In contrast to
Meissner et al. [2007], we here find that a deep convection event during a transient high CO₂ emission scenario can result in
carbon uptake, as also found in CMIP5 model runs [Bernardello et al., 2014]. This can be explained by the fact that the pCO₂
of the old (pre-industrial) water masses that reach the surface during deep convection is lower than the atmospheric pCO₂ in
305 the I-1500 simulation at the end of the 22nd century. Compared to the injected carbon content of 70 GtC at the end of the
injection period, the deep convection event leads to a significant carbon uptake of about 19 %. Compared to the oceanic
uptake of anthropogenic CO₂ by the end of the simulation, the carbon uptake associated with the deep convection event
amounts to less than 1 %. The deep convection event also causes the ocean to lose a substantial amount of heat, which
causes regional warming and thus partially counteracts the cooling effect associated with the direct CO₂ injection in I-1500.
310 This is also reflected in a slower increase in total land carbon (Fig. 4 e, f) through more soil respiration than in I-800 and I-
3000.

Recurring open ocean deep convection in the Southern Ocean has been found in many CMIP5 models (Lavergne et
al., 2014) and also in the Kiel Climate Model, for which the driving mechanism could be linked to internal climate
variability [Martin et al., 2013]. Although the modeled deep convection events feature similarities to processes associated
315 with the Weddell Polyna of the 1970s [Martin et al., 2013], uncertainty remains regarding their realism. An important model
constraint in this respect is a coarse grid resolution, which hinders, for instance, the correct representation of bottom water
formation processes on the continental shelf and instead might favor open-ocean deep convection [Bernardello et al., 2014].

It is intriguing that among thirteen millennial-scale simulations performed for this study, a deep convection event
occurred only in three simulations, the I-1500, an injection run with a ten year injection period (not shown) and the DAC



320 run. Apparently, small internal variability combined with certain CO₂ levels can give rise to such events [Meissner et al.,
2007]. The only means to discriminate between the feedbacks of the ocean deep convection event, which are driven by little
internal variability in the UVic model, would be to run ensembles with different initial conditions. This is how one would
also discriminate between other feedbacks and internal variability in models with more intense –and more realistic– levels of
internal variability. Such open-ocean deep convection can cause an inter-model spread in projections of future ocean carbon
325 uptake [Bernardello et al., 2014] and may make accounting for the injected CO₂ as the net fraction stored (*netFS*) very
difficult. As shown by the dashed lines in Figure 4, the fraction of the injected CO₂ retained (*FR*), that could in principle be
tracked via a marker tracer, is more robust to internal variability of the model and, presumably, of the real world. A
pragmatic and robust way to account for the storage of injected CO₂ might therefore well be based on *FR* despite its neglect
of carbon cycle and climate feedbacks. To account for these feedbacks, *FR* could possibly be augmented by some model-
330 derived correction factors to account for the ensemble-averaged interaction of the ocean with the other carbon pools under
changing climate conditions.

4. Conclusions

We use an Earth System Model of intermediate complexity to simulate direct CO₂ injections into the deep ocean under a high
CO₂ emission scenario. The model-predicted fractions retained (*FR*) are found to be within the range of the values found by
335 Orr et al. [2001]. In agreement with earlier studies [Jain and Cao, 2005] we also find that the *FR* is enhanced as global
warming progresses. In our simulations, this enhancement amounts to about 7% to 16% at the end of the simulations (year
3020). Injection sites in the Pacific are the most effective ones on the millennial time scale considered in our simulations.

The response of the carbon cycle during and after the injections is dominated by the partial outgassing of injected
CO₂ and a reduced rate of air-sea gas exchange compared to the control run without injection. Relative to the control run, the
340 model's terrestrial ecosystems respond to the marine CO₂ injection and reduced atmospheric CO₂ concentrations via a
reduced CO₂ fertilization effect and a temperature-related decrease in soil respiration. This leads to a maximum reduction in
total land carbon by about 4 GtC (relative to the control run) during the injection period in all WE simulations (Fig. 4 e).
After the injection period, total land carbon becomes higher than in the control simulation, mainly due to a terrestrial carbon
cycle-climate feedback, with a maximum increase of about 5 GtC for I-3000 in the year 2230 (Fig. 4 e). The influence of the



345 highly uncertain carbon-cycle and climate feedbacks in our findings, in addition to the sporadic deep convection event in I-
1500, illustrates the difficulty of quantitatively detecting, attributing, and eventually accounting for, carbon storage and
carbon fluxes generated by individual carbon sequestration measures even in relatively coarse-resolution models with little
internal climate variability (“noise”). Nevertheless, our findings show the importance of accounting for all carbon fluxes in
the carbon cycle and not only for those of the manipulated reservoir, to obtain a comprehensive assessment of direct oceanic
350 CO₂ injection in particular and carbon sequestration in general.

355

360

365



370 **Acknowledgments**

The model data used to generate the table and figures will be available at

<http://thredds.geomar.de/thredds/catalog-opene-access.html>.

The Deutsche Forschungsgemeinschaft (DFG) financially supported this study via the Priority Program 1689. We thank Torge Martin, Wolfgang Koeve, Nadine Mengis, Julia Getzlaff, Levin Nickelsen, Peter Vandromme, Markus Pahlow, Wilfried Rickels and Ell Yuming Feng for their thoughtful discussions and advice.

380

385

390



395 References

- Ahlström, A., Schurgers, G., Arneeth, A. and Smith, B.: Robustness and uncertainty in terrestrial ecosystem carbon response to CMIP5 climate change projections, *Environ. Res. Lett.*, 7(4), 044008, doi:10.1088/1748-9326/7/4/044008, 2012.
- Archer, D., Eby, M., Brovkin, V., Ridgwell, A., Cao, L., Mikolajewicz, U., Caldeira, K., Matsumoto, K., Munhoven, G., Montenegro, A. and Tokos, K.: Atmospheric Lifetime of Fossil Fuel Carbon Dioxide, *Annu. Rev. Earth Planet. Sci.*, 37(1), 400 117–134, doi:10.1146/annurev.earth.031208.100206, 2009.
- Arora, V. K., Boer, G. J., Friedlingstein, P., Eby, M., Jones, C. D., Christian, J. R., Bonan, G., Bopp, L., Brovkin, V., Cadule, P., Hajima, T., Ilyina, T., Lindsay, K., Tjiputra, J. F. and Wu, T.: Carbon–Concentration and Carbon–Climate Feedbacks in CMIP5 Earth System Models, *J. Clim.*, 26(15), 5289–5314, doi:10.1175/JCLI-D-12-00494.1, 2013.
- Bernardello, R., Marinov, I., Palter, J. B., Galbraith, E. D., and Sarmiento, J. L.: Impact of Weddell Sea deep convection on natural and anthropogenic carbon in a climate model, *Geophys. Res. Lett.*, 41, doi:10.1002/2014GL061313, 2014.
- 405
- Bitz, C. M. and Lipscomb, W. H.: An energy-conserving thermodynamic model of sea ice, *J. Geophys. Res.*, 104(C7), 15669, doi:10.1029/1999JC900100, 1999.
- Bopp, L., Resplandy, L., Orr, J. C., Doney, S. C., Dunne, J. P., Gehlen, M., Halloran, P., Heinze, C., Ilyina, T., Séférian, R., Tjiputra, J., and Vichi, M.: Multiple stressors of ocean ecosystems in the 21st century: projections with CMIP5 models, 410 *Biogeosciences*, 10, 6225–6245, doi:10.5194/bg-10-6225-2013, 2013.
- Cao, L. and Caldeira, K.: Atmospheric carbon dioxide removal: long-term consequences and commitment, *Environ. Res. Lett.*, 5(2), 024011, doi:10.1088/1748-9326/5/2/024011, 2010.
- Carvalhais, N., Forkel, M., Khomik, M., Bellarby, J., Jung, M., Migliavacca, M., Mingquan, M., Saatchi, S., Santoro, M., Thurner, M., Weber, U., Ahrens, B., Beer, C., Cescatti, A., Randerson, J. T. and Reichstein, M.: Climate in Terrestrial 415 *Ecosystems*, *Nature*, 514(7521), 213–217, doi:10.1038/nature13731, 2014.
- DeVries, T. and Primeau, F.: Dynamically and Observationally Constrained Estimates of Water-Mass Distributions and Ages in the Global Ocean, *J. Phys. Oceanogr.*, 41(12), 2381–2401, doi:10.1175/JPO-D-10-05011.1, 2011.



- Doney, S. C.: The growing human footprint on coastal and open-ocean biogeochemistry., *Science*, 328(5985), 1512–6, doi:10.1126/science.1185198, 2010.
- 420Eby, M., Weaver, a. J., Alexander, K., Zickfeld, K., Abe-Ouchi, A., Cimatoribus, A. A., Crespin, E., Drijfhout, S. S., Edwards, N. R., Eliseev, A. V., Feulner, G., Fichet, T., Forest, C. E., Goosse, H., Holden, P. B., Joos, F., Kawamiya, M., Kicklighter, D., Kienert, H., Matsumoto, K., Mokhov, I. I., Monier, E., Olsen, S. M., Pedersen, J. O. P., Perrette, M., Philippon-Berthier, G., Ridgwell, A., Schlosser, A., Von Deimling, T. S., Shaffer, G., Smith, R. S., Spahni, R., Sokolov, A. P., Steinacher, M., Tachiiri, K., Tokos, K., Yoshimori, M., Zeng, N. and Zhao, F.: Historical and idealized climate model
425 experiments: An intercomparison of Earth system models of intermediate complexity, *Clim. Past*, 9(3), 1111–1140, doi:10.5194/cp-9-1111-2013, 2013.
- Fanning, A. F. and Weaver, A. J.: An atmospheric energy-moisture balance model: Climatology, interpentadal climate change, and coupling to an ocean general circulation model, *J. Geophys. Res.*, 101(D10), 15111, doi:10.1029/96JD01017, 1996.
- Friedlingstein, P., Andrew, R. M., Rogelj, J., Peters, G. P., Canadell, J. G., Knutti, R., Luderer, G., Raupach, M. R., Schaeffer,
430 M., Vuuren, D. P. Van and Quéré, C. Le: Persistent growth of CO₂ emissions and implications for reaching climate targets, *Nat. Publ. Gr.*, 7(10), 709–715, doi:10.1038/ngeo2248, 2014.
- Hagerty, S. B., van Groenigen, K. J., Allison, S. D., Hungate, B. A., Schwartz, E., Koch, G. W., Kolka, R. K. and Dijkstra, P.: Accelerated microbial turnover but constant growth efficiency with warming in soil, *Nat. Clim. Chang.*, (September), 3–6, doi:10.1038/nclimate2361, 2014.
- 435Hoffert, M. I., Wey, Y. C., Callegari, A. J. and Broecker, W. S.: Atmospheric response to deep-sea injections of fossil-fuel carbon dioxide, *Clim. Change*, 2(1), 53–68, doi:10.1007/BF00138226, 1979.
- Intergovernmental Panel on Climate Change (IPCC), [Metz, B., Davidson, O., de Coninck, H. C., Loos, M., and Meyer, L. A. (eds.)]: *Special Report on Carbon Dioxide Capture and Storage*, Cambridge University Press, Cambridge, United Kingdom and New York, NY, USA, 422pp., 2005.
- 440Jain, A. K.: Assessing the effectiveness of direct injection for ocean carbon sequestration under the influence of climate change, *Geophys. Res. Lett.*, 32(9), L09609, doi:10.1029/2005GL022818, 2005.



- Keller, D. P., Oschlies, A. and Eby, M.: A new marine ecosystem model for the University of Victoria Earth System Climate Model, *Geosci. Model Dev.*, 5(5), 1195–1220, doi:10.5194/gmd-5-1195-2012, 2012.
- Keller, D. P., Feng, E. Y. and Oschlies, A.: Potential climate engineering effectiveness and side effects during a high carbon dioxide-emission scenario, *Nat Commun*, 5 [online] Available from: <http://dx.doi.org/10.1038/ncomms4304>, 2014.
- Lavergne, C. De, Palter, J. B., Galbraith, E. D., Bernardello, R. and Marinov, I.: Cessation of deep convection in the open Southern Ocean under anthropogenic climate change, , (April), 0–4, doi:10.1038/NCLIMATE2132, 2014.
- Leung, D. Y. C., Caramanna, G. and Maroto-Valer, M. M.: An overview of current status of carbon dioxide capture and storage technologies, *Renew. Sustain. Energy Rev.*, 39, 426–443, doi:10.1016/j.rser.2014.07.093, 2014.
- 450 Marchetti, C.: On geoengineering and the CO₂ problem, *Clim. Change*, 1(1), 59–68, doi:10.1007/BF00162777, 1977.
- Martin, T., Park, W. and Latif, M.: Multi-centennial variability controlled by Southern Ocean convection in the Kiel Climate Model, *Clim. Dyn.*, 40(7-8), 2005–2022, doi:10.1007/s00382-012-1586-7, 2013.
- Matthews, H. D.: Implications of CO₂ fertilization for future climate change in a coupled climate-carbon model, *Glob. Chang. Biol.*, 13(5), 1068–1078, doi:10.1111/j.1365-2486.2007.01343.x, 2007.
- 455 Meinshausen, M., Smith, S. J., Calvin, K., Daniel, J. S., Kainuma, M. L. T., Lamarque, J., Matsumoto, K., Montzka, S. A., Raper, S. C. B., Riahi, K., Thomson, A., Velders, G. J. M. and van Vuuren, D. P. P.: The RCP greenhouse gas concentrations and their extensions from 1765 to 2300, *Clim. Change*, 109(1), 213–241, doi:10.1007/s10584-011-0156-z, 2011.
- Meissner, K. J., Weaver, A. J., Matthews, H. D. and Cox, P. M.: The role of land surface dynamics in glacial inception: A study with the UVic Earth System Model, *Clim. Dyn.*, 21(7-8), 515–537, doi:10.1007/s00382-003-0352-2, 2003.
- 460 Meissner, K. J., Eby, M., Weaver, A. J. and Saenko, O. A.: CO₂ threshold for millennial-scale oscillations in the climate system: implications for global warming scenarios, *Clim. Dyn.*, 30(2-3), 161–174, doi:10.1007/s00382-007-0279-0, 2007.
- Mueller, K., Cao, L., Caldeira, K. and Jain, A.: Differing methods of accounting ocean carbon sequestration efficiency, *J. Geophys. Res. C Ocean.*, 109, 1–7, doi:10.1029/2003JC002252, 2004.



- 465Orr, J. C., Najjar, C. R., Sabine, C. L., and Joos, F.: Abiotic-Howto. Internal OCMIP Report, LCSE/CEA Saclay, Gif-sur-Yvette, France, 25pp, 1999.
- Orr, J. C., Aumont, O., Yool, A., Plattner, K., Joos, F., Maier-Reimer, E., Weirig, M. -F., Schlitzer, R., Caldeira, K., Wicket, M., and Matear, R.: Ocean CO₂ Sequestration Efficiency from 3-D Ocean Model Comparison, in Greenhouse Gas Control Technologies), edited by Williams, D., Durie, B., McMullan, P., Paulson, C., and Smith, A., CSIRO, Collingwood, Australia, 470 pp. 469-474, 2001.
- Orr, J. C.: Modelling of ocean storage of CO₂ - The GOSAC study, Report PH4/37, IEA Greenhouse gas R&D Programme, 96pp., 2004.
- Oschlies, A., Pahlow, M., Yool, A. and Matear, R. J.: Climate engineering by artificial ocean upwelling: Channelling the sorcerer's apprentice, *Geophys. Res. Lett.*, 37(4), n/a–n/a, doi:10.1029/2009GL041961, 2010.
- 475Pacanowski, R. C.: MOM2: Documentation, User's Guide and Reference Manual, GFDL Ocean Tech. Rep., 3.2, 329pp, 1996.
- Prentice, I. C, Farquhar, G. D., Fasham, M. J. R., Goulden, M.L., Heimann, M., Jaramillo, V. J., Kheshgi, H. S., Le Quéré, C., Scholes, R. J. and Wallace, D. W. R.: The carbon cycle and atmospheric carbon dioxide, in *Climate Change 2001: The Scientific Basis: Contribution of Working Group I to the Third Assessment Report of the Intergovernmental Panel on Climate Change*, edited by J. T. Houghton et al., 881 pp., Cambridge Univ. Press, New York, 2001.
- 480Peters, G.P., Andrew, R. M., Boden, T., Canadell, J. G., Ciais, P., Le Quéré, C., Marland, G., Raupach, M. R., and Wilson, C.: The challenge to keep global warming below 2[deg]C, *Nat. Clim. Chang.*, 3(1),4-6, doi:10.1038/nclimate1783, 2013
- Le Quéré, C., Peters, G. P., Andres, R. J., Andrew, R. M., Boden, T. A., Ciais, P., Friedlingstein, P., Houghton, R. A., Marland, G., Moriarty, R., Sitch, S., Tans, P., Arneeth, A., Arvanitis, A., Bakker, D. C. E., Bopp, L., Canadell, J. G., Chini, L. P., Doney, S. C., Harper, A., Harris, I., House, J. I., Jain, A. K., Jones, S. D., Kato, E., Keeling, R. F., Klein Goldewijk, K., 485 Körtzinger, A., Koven, C., Lefèvre, N., Maignan, F., Omar, A., Ono, T., Park, G. H., Pfeil, B., Poulter, B., Raupach, M. R., Regnier, P., Rödenbeck, C., Saito, S., Schwinger, J., Segschneider, J., Stocker, B. D., Takahashi, T., Tilbrook, B., Van Heuven, S., Viovy, N., Wanninkhof, R., Wiltshire, A. and Zaehle, S.: Global carbon budget 2013, *Earth Syst. Sci. Data*, 6, 235–263, doi:10.5194/essd-6-235-2014, 2014.



- Ridgwell, A., Rodengen, T. J. and Kohfeld, K. E.: Geographical variations in the effectiveness and side effects of deep ocean
490 carbon sequestration, *Geophys. Res. Lett.*, 38(17), 1–6, doi:10.1029/2011GL048423, 2011.
- Rogelj, J., Chen, C., Nabel, J., Macey, K., Hare, W., Schaeffer, M., Markmann, K., Höhne, N., Krogh Andersen, K. and
Meinshausen, M.: Analysis of the Copenhagen Accord pledges and its global climatic impacts—a snapshot of dissonant
ambitions, *Environ. Res. Lett.*, 5(3), 034013, doi:10.1088/1748-9326/5/3/034013, 2010.
- Schimel, D., Stephens, B. B. and Fisher, J. B.: Effect of increasing CO₂ on the terrestrial carbon cycle, *Proc. Natl. Acad. Sci.*,
495 112, 436–441, doi:10.1073/pnas.1407302112, 2015.
- Shepherd, J. G.: *Geoengineering the climate: Science, governance and uncertainty.*, 2009.
- Sun, Y., Gu, L., Dickinson, R. E., Norby, R. J., Pallardy, S. G. and Hoffman, F. M.: Impact of mesophyll diffusion on estimated
global land CO₂ fertilization, *Proc. Natl. Acad. Sci.*, doi:10.1073/pnas.1418075111, 2014.
- UNFCCC. Conference of the Parties: Adoption of the Paris Agreement. Proposal by the President., *Paris Clim. Chang. Conf.*
500 Novemb. 2015, COP 21, 21930 (December 2015), 31 [online] Available from:
<http://unfccc.int/resource/docs/2015/cop21/eng/l09.pdf>, 2015.
- Van der Sleen, P., Groenendijk, P., Vlam, M., Anten, N. P. R., Boom, A., Bongers, F., Pons, T. L., Terburg, G. and Zuidema, P.
A.: No growth stimulation of tropical trees by 150 years of CO₂ fertilization but water-use efficiency increased, *Nat. Geosci.*,
(December 2014), 1–5, doi:10.1038/ngeo2313, 2014.
- 505 Vichi, M., Navarra, A. and Fogli, P. G.: Adjustment of the natural ocean carbon cycle to negative emission rates, *Clim. Change*,
118(1), 105–118, doi:10.1007/s10584-012-0677-0, 2013.
- Weaver, A. J., Eby, M., Wiebe, E. C., Bitz, C. M., Duffy, P. B., Ewen, T. L., Fanning, A. F., Holland, M. M., MacFadyen, A.,
Matthews, H. D., Meissner, K. J., Saenko, O., Schmittner, A., Wang, H. and Yoshimori, M.: The UVic earth system climate
model: Model description, climatology, and applications to past, present and future climates, *Atmosphere-Ocean*, 39(4),
510 361–428, doi:10.1080/07055900.2001.9649686, 2001.
- Zickfeld, K., Eby, M., Weaver, A. J., Alexander, K., Crespin, E., Edwards, N. R., Eliseev, A. V., Feulner, G., Fichefet, T.,



515 Forest, C. E., Friedlingstein, P., Goosse, H., Holden, P. B., Joos, F., Kawamiya, M., Kicklighter, D., Kienert, H., Matsumoto,
K., Mokhov, I. I., Monier, E., Olsen, S. M., Pedersen, J. O. P., Perrette, M., Philippon-Berthier, G., Ridgwell, A., Schlosser,
A., Schneider Von Deimling, T., Shaffer, G., Sokolov, A., Spahni, R., Steinacher, M., Tachiiri, K., Tokos, K. S., Yoshimori,
520 M., Zeng, N. and Zhao, F.: Long-Term Climate Change Commitment and Reversibility: An EMIC Intercomparison, *J. Clim.*,
26(16), 5782–5809, doi:10.1175/JCLI-D-12-00584.1, 2013.

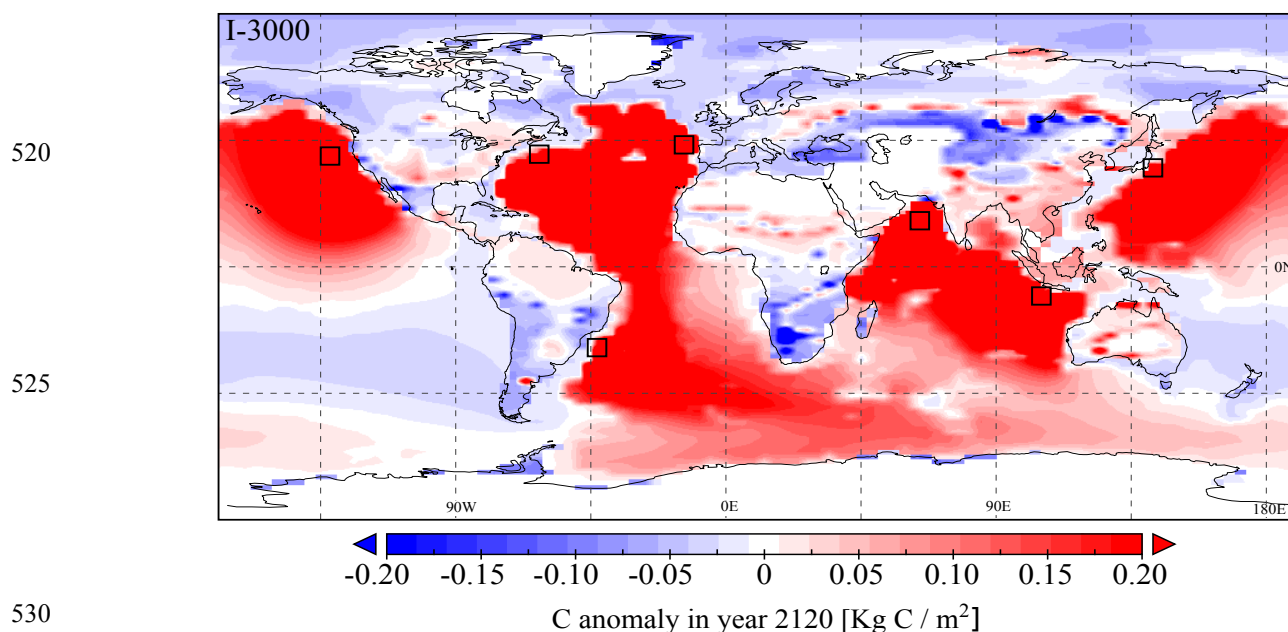


Figure 1: Absolute changes in oceanic and land carbon between I-3000 and the RCP 8.5 control run (I-3000 simulation minus RCP 8.5 control run) at the end of the injection period (year 2120). The black rectangles represent the locations of the seven injection sites, where the injections occurred in the center of the black rectangles.

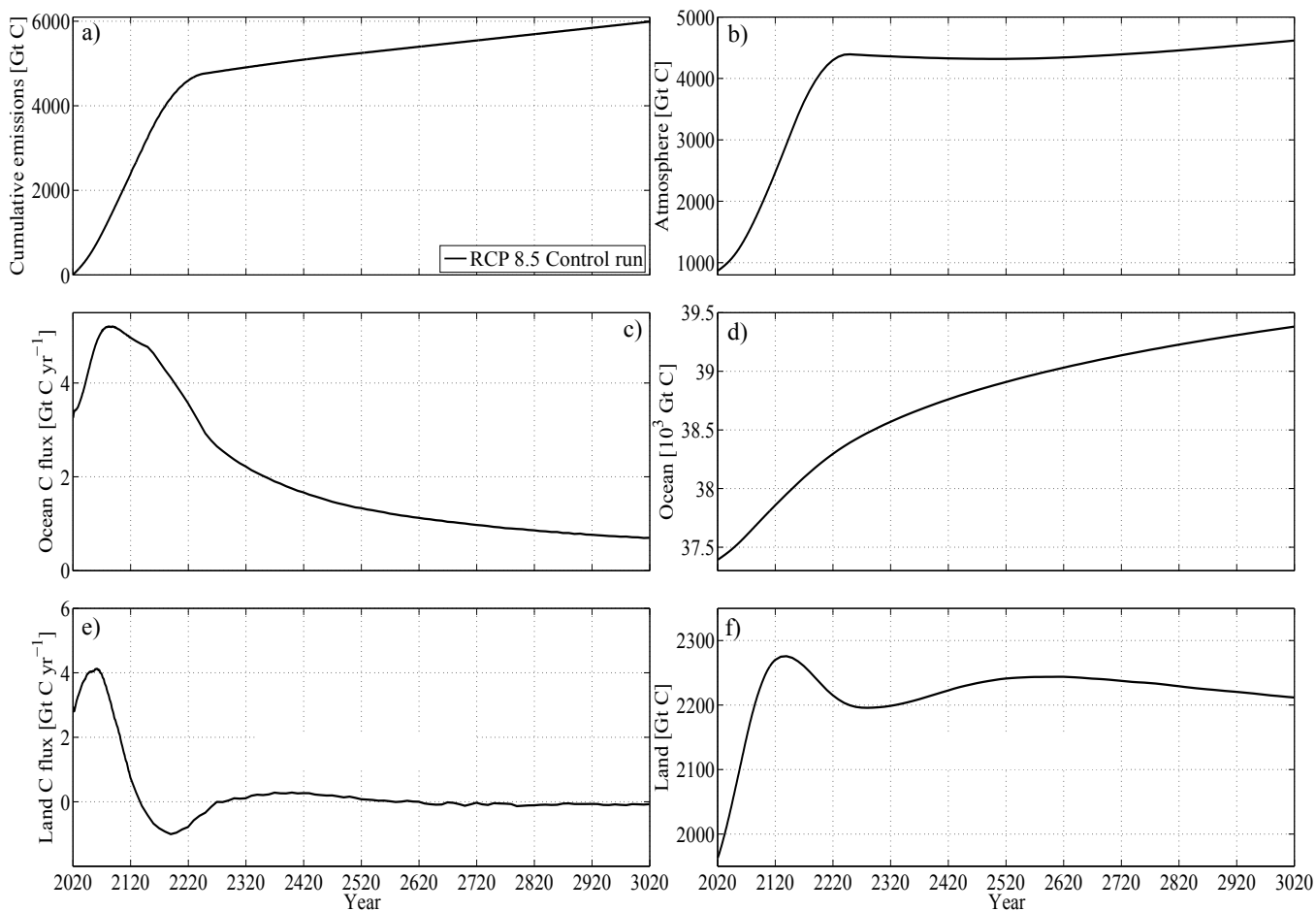


Figure 2: (a) Cumulative CO₂ emissions of the RCP 8.5 and globally integrated carbon of the RCP 8.5 control run for (b) total atmospheric carbon, (c) carbon flux from atmosphere to ocean, (d) total oceanic carbon, (e) carbon flux from atmosphere to land, (f) total land carbon

545

550



555

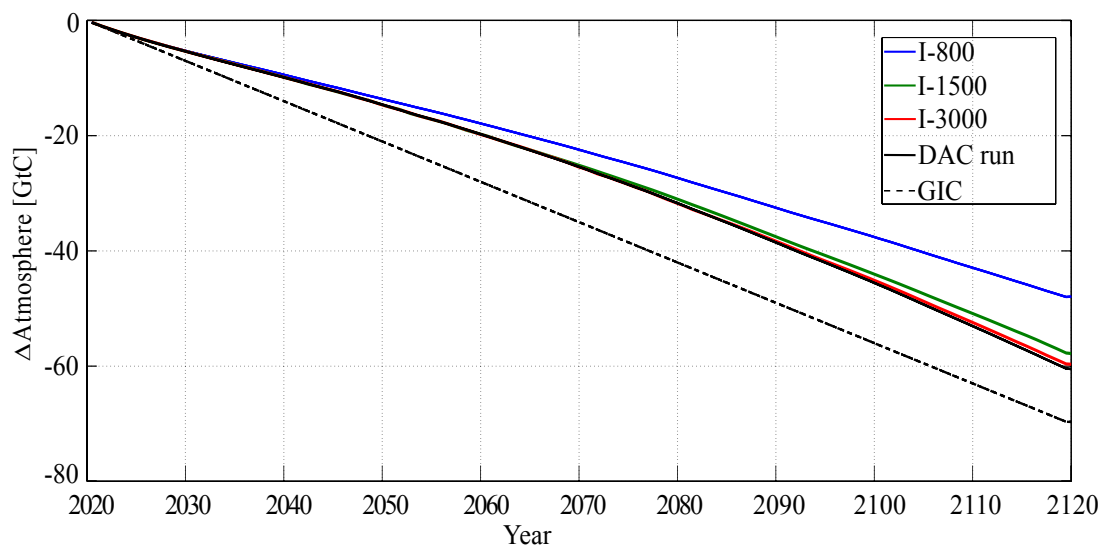
Table 1: Comparison of fractions retained (*FR*) between Orr et al. [2001; Orr, 2004] (Full Range of their Global Efficiency, which is the same as the *FR* defined in section 2.2 and is based on seven OGCM and one zonally averaged model results) and our CM and WE simulations for all injection sites (Global) and on an inter-basin level for the Atlantic sites (Bay of Biscay, New York, Rio de Janeiro), the Pacific sites (San Francisco, Tokyo) and the Indian sites (Jakarta, Mumbai). The *FR* values [%] are given for the last year of the injections (2119), 500 years after the simulations started (2519) and for the last year of the simulations (3019). For each entry of the table, numbers to the left of the vertical bar denote results of the CM runs, numbers to the right results of the WE runs. Note that the illustrated years refer to our simulations, ranging from year 2020 until the year 3020. The GOSAC-OCMIP simulations started in the year 2000 and ended in the year 2500 [Orr et al., 2001].

Overview of FR [%]	I-800			I-1500			I-3000		
	Year			Year			Year		
	2119	2519	3019	2119	2519	3019	2119	2519	3019
Full Range [Orr et al., 2001; Orr, 2004]	65 - 84	15 - 38	-	81 - 96	32 - 57	-	97 - 100	49 - 93	-
CM WE Global	68 75	17 30	8 17	92 95	40 56	20 35	99 100	65 76	38 54
CM WE Atlantic sites (70°N:35°S)	53 64	9 20	5 11	85 91	30 46	16 28	97 99	62 75	37 54
CM WE Pacific sites (65°N:35°S)	78 81	27 45	13 29	97 98	61 77	34 55	99 100	86 93	59 75
CM WE Indian sites (20°N:35°S)	80 84	17 29	6 14	96 97	34 49	13 25	99 100	50 65	20 34

560



565



570

Figure 3: Absolute change in atmospheric carbon in the DAC run and in the WE simulations, relative to the RCP8.5 control run. The black dashed line denotes the globally injected carbon, which is subtracted from the emission forcing (see section 2.2).

575

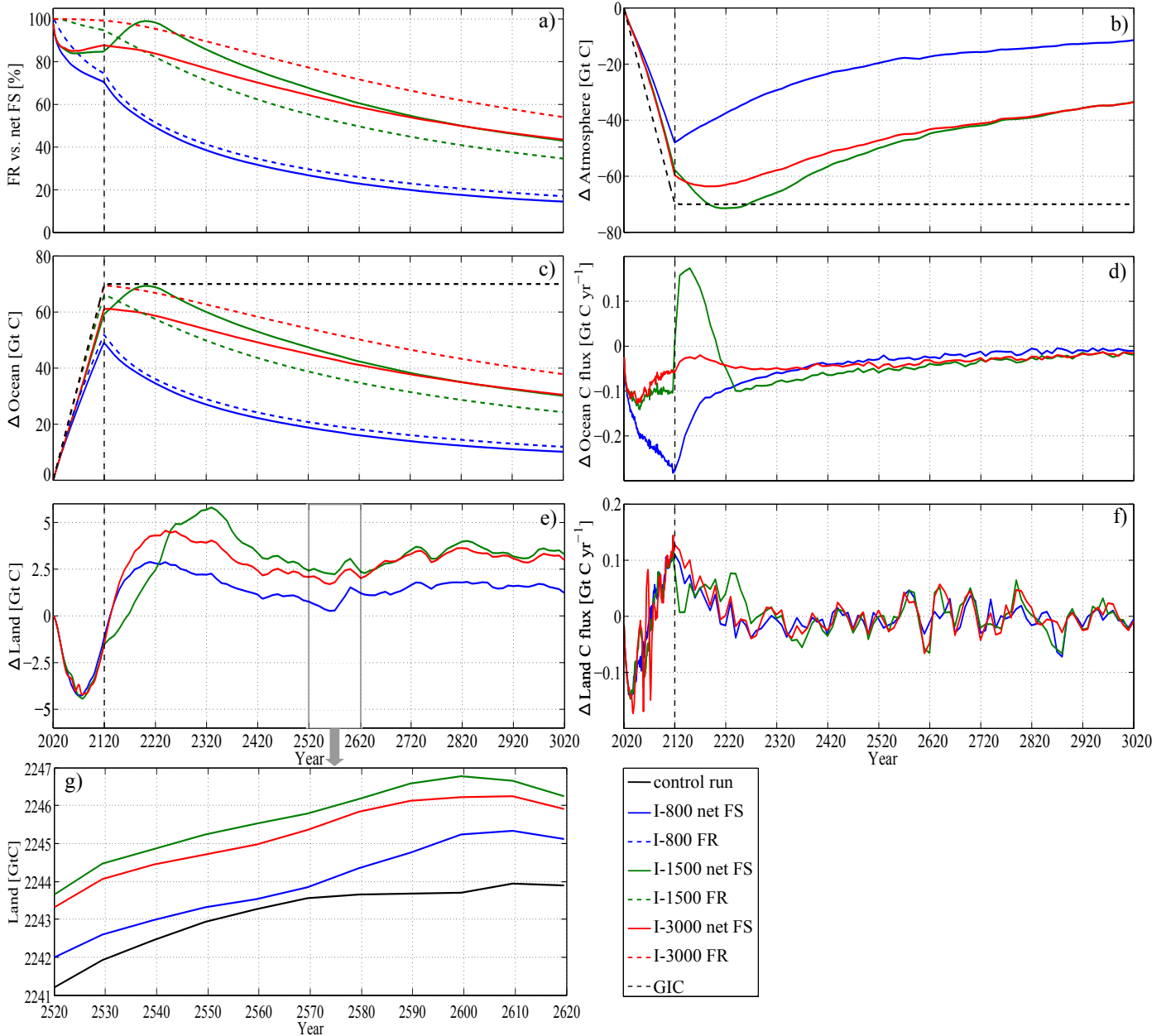


Figure 4: (a) Comparison of the fractions retained (*FR*, dashed) and the net fractions stored (*netFS*, solid) of the WE simulations. Absolute changes in carbon between the WE simulations and the RCP 8.5 control simulation (WE simulations minus RCP 8.5 control run) or (b) globally integrated total atmospheric carbon, (c) globally integrated total oceanic carbon, (d) globally integrated carbon flux from atmosphere to ocean, (e) globally integrated total land carbon, (f) globally integrated carbon flux from atmosphere to land, and (g) absolute values of globally integrated total land carbon of the WE simulations and the RCP 8.5 control run from year 2520 to 2620. The vertical dashed black lines indicate the end of the injection period.